

# Cystamindi-ium tetrachlorocuprate $[\text{NH}_3(\text{CH}_2)_2\text{SS}(\text{CH}_2)_2\text{NH}_3][\text{CuCl}_4]$ : synthesis, crystal structure, and thermal decomposition

D. Y. Leshok, N. N. Golovnev, and S. D. Kirik<sup>a)</sup>

Siberian Federal University, 660041, Krasnoyarsk, 79 Svobodny av., Russian Federation

(Received 15 May 2014; accepted 8 December 2014)

The salt  $[\text{NH}_3(\text{CH}_2)_2\text{SS}(\text{CH}_2)_2\text{NH}_3][\text{CuCl}_4]$  was obtained by crystallization after adding  $\text{CuCl}_2$  to cystamine (Cysta), solved in hydrochloric acid. The assumption of conserved disulfide connection (S–S) in the compound, made on the basis of infrared spectroscopy, is further supported by the crystal structure determined from X-ray powder diffraction data. The compound has an ionic structure.  $[\text{CuCl}_4]^{2-}$  and  $\text{CystaH}_2^{2+}$  ions package in the form of inorganic and organic layers in the cell, interconnected through the formation of hydrogen bonds via  $\text{NH}_3$ -groups and chlorine atoms of the complex  $[\text{CuCl}_4]^{2-}$ . Inorganic layers are additionally stabilized in the parquet package of  $[\text{CuCl}_4]^{2-}$  ions which provides a Cu-distorted octahedral coordination.  $\text{CystaH}_2[\text{CuCl}_4]$  is stable in air up to 200 °C. Thermal decomposition occurs in several stages, accompanied by breaking of S–S bonds, releasing of the organic component and yielding  $\text{CuO}$ . © 2015 International Centre for Diffraction Data. [doi:10.1017/S0885715614001390]

Key words: copper dichloride ( $\text{CuCl}_2$ ), cystamine, disulfide, X-ray powder crystal structure determination, thermal analysis

Coordination chemistry of sulfur in biological systems attracts a lot of attention (Allegra *et al.*, 2002). One of the reasons is that the redox equilibrium between organic disulfides  $\text{R–SS–R}$  and mercaptides  $\text{RS–}$  can be shifted by complexation of the organic molecules by metal ions (Eremin *et al.*, 2009). For instance, the cysteine moieties were involved in mercury ion binding in the regulatory protein MerR (Wilson *et al.*, 2000), MerP (Steele and Opella, 1997). Numerous works were devoted to investigations of cysteine activity with metals in biological systems (Shaw *et al.*, 1991). In contrast, the chemistry of cysteamine  $\text{HS}(\text{CH}_2)_2\text{NH}_2$  (Cystea), containing a similar sulfur moiety, has not been studied deeply enough, despite the fact that this compound was used in many medications. One of the significant cysteamine application is the use as an effective radioprotective agent (Mark *et al.*, 1982). In medicine cysteamine is also used for the treatment of cystinosis disease. Its activity is reduced by binding an excess of intracellular cysteine into soluble cysteine–cysteamine complex which then is removed from the body (Markello *et al.*, 1993). It is well known that there is the redox equilibrium between cysteamine and cystamine  $\text{NH}_2(\text{CH}_2)_2\text{SS}(\text{CH}_2)_2\text{NH}_2$  (Cysta) in the body. In cells, these compounds coexist simultaneously and, consequently, their metabolisms are closely related, as well as biological functions. Mutual transformation “Cystea  $\leftrightarrow$  Cysta” could be influenced by metal ions, solution composition, and acidity.

The breaking S–S bond in cystamine with the formation of cysteamine was observed at synthesis  $[\text{Ni}(\text{Cystea})_2]\text{Cl}_2$  and  $[\text{Cu}(\text{Cystea})_2]\text{Cl}_2$  (Carrillo *et al.*, 1989). The phenomenon was also observed at the formation of  $[\text{Hg}(\text{Cystea})_2]\text{Cl}_2$  at 4 °C (Kim *et al.*, 2002). The salts of Pd(II) and Pt(II) give cysteamine

complexes both in strong acidic and alkaline media (Foye and Kaewchansilp, 1979). There are a number of cases where S–S bond in cystamine is left intact when using organic solvents. For example, the  $\text{PbX}_2$  (where  $X = \text{Br}, \text{I}$ ) interacts with cystamindi-ium dihydrochloride in  $\text{CH}_3\text{CN}$  giving  $\text{CystaH}_2[\text{PbX}_4]$  (Louvain *et al.*, 2007). The  $\text{CystaH}_2[\text{HgCl}_4]$  was obtained under neutral conditions in a nitrogen stream (Bharara *et al.*, 2005a). There are other ionic compounds containing cystamindi-ium cation, for example, with bismuth  $\text{CystaH}_2[\text{Bi I}_5]$ ,  $(\text{CystaH}_2)_2\text{I}_3[\text{Bi I}_6]$  (Bi *et al.*, 2007, 2008) and with vanadium  $(\text{CystaH}_2)_2\text{H}_2[\text{V}_{10}\text{O}_{28}] \cdot 4\text{H}_2\text{O}$ ,  $(\text{CystaH}_2)_5\text{H}_4[\text{V}_{15}\text{O}_{42}]_2 \cdot 10\text{H}_2\text{O}$  (Pavani *et al.*, 2006). As a rule, cystamindi-ium cations occupy crystalline space by individual particles linking with an anionic part by the Coulomb forces and hydrogen bonds. The anionic part can be fulfilled by the local anions or polyanions and infinite ribbon-like or planar polymers. It is interesting to note that plumbate and bismuthate of cystamindi-ium exhibit nonlinear optical properties (the generation of the second harmonic) and can be interesting from the material science point of view (Louvain *et al.*, 2007). It is assumed that the NLO property is because of acentric geometry of cystamindi-ium cation. Dihedral angle C–S–S–C in the ion at approximately 90° excludes symmetry center in the cation. In the case of copper(I), there are known two compounds  $\text{CystaH}_2[\text{Cu}_2\text{Br}_4]$  and  $\text{CystaH}_2[\text{Cu}_3\text{Br}_5]$ , and the first one has two crystal modifications (Louvain *et al.*, 2008). Cu(I) exhibits the specific interaction with cystamindi-ium. It is coordinated by two sulfur atoms of cystamindi-ium cation. As a result copper atom reconstructs its linear coordination into more saturated tetrahedral one.

In the present paper, the reaction of cystamindi-ium dihydrochloride  $\text{CystaH}_2\text{Cl}_2$  with  $\text{CuCl}_2$  in a strongly acidic medium (10 M HCl) has been studied. It was interesting to clear up the S–S bond behavior and coordination mode of Cu(II). The resulting substance  $\text{CystaH}_2[\text{CuCl}_4]$  was studied by thermal

<sup>a)</sup> Author to whom correspondence should be addressed. Electronic mail: Kiriksd@yandex.ru

analysis and infrared (IR) spectroscopy. As the substance was available in the form of fine powder, the crystal structure determination was carried out using X-ray powder diffraction technique.

## I. EXPERIMENTAL

### A. Synthesis

For  $\text{CystaH}_2[\text{CuCl}_4]$  synthesis 2 ml concentrated HCl (10 M) was added to 0.20 g  $\text{CystaH}_2\text{Cl}_2$ , and the dry salt  $\text{CuCl}_2$  in the ratio  $\text{Cu(II)}:\text{CystaH}_2$  more than 2:1 was dissolved in the resulting solution. After 3 days the yellow precipitate crystallized from the solution. It was filtered, washed with acetone, and left to dry in air at room temperature. Yield was 60–70%. The product can be decomposed in water.

### B. Thermal-, HCN- analysis, and IR spectra registration

Thermal analysis was done on NETZSCH409 in air, heating rate was  $10\text{ }^\circ\text{C min}^{-1}$ , temperature range was 23–700  $^\circ\text{C}$ , and the sample weight was 10–15 mg. IR spectra were recorded in the 400–4000  $\text{cm}^{-1}$  region as KBr (0.1%) pellets on FTIR Nicolet 6700 IR spectrophotometer. IR spectrum (KBr,  $\text{v, cm}^{-1}$ ): 3104, 2947, 2611, 2406, 1564, 1479, 1462, 1444, 1407, 1379, 1320, 1257, 1246, 1228, 1126, 1087, 1055, 1021, 935, 917, 868, 802, 781, 734, 632, 461. The chemical analysis was carried out with the C,H,N-analyzer: EURO EA Elemental Analyzer. Chemical composition, found: C 13.01%, H 4.32%, N 7.36%, S 17.56%, Cu 17.06%; calculated: C 13.36%, H 3.92%, N 7.79%, S 17.83%, Cu 17.67%.

### C. X-ray powder diffraction study

Crystal structure determination  $\text{CystaH}_2[\text{CuCl}_4]$  was carried out using X-ray powder diffraction data. Experimental data were obtained on X'Pert PRO diffractometer (PANalytical) with a PIXcel detector, equipped with a graphite monochromator.  $\text{CuK}\alpha$  radiation was applied. The sample was prepared in a cuvette of 25 mm in diameter by means of direct loading. The unit-cell parameters were defined using the programs (Visser, 1969; Kirik *et al.*, 1981). The space group followed from regular reflection absence. The structural models were determined in the direct space applying the “simulated annealing” approach (Solovyov and Kirik, 1993) with the program FOX (Favre-Nicolin and Černý, 2002). The square planar anionic complex  $[\text{CuCl}_4]^{2-}$  with the regular geometry and cystamindi-ium ion with the standard configuration were the basic molecular particles for the structure modeling. Actually the structure determination consisted in finding an optimal positions and orientations of the molecular particles in the space of a unit cell. The most optimal structural model was refined by the full-profile technique (Rietveld method) using the program FullProf (Rodriguez-Carvajal, 2009). Rigid and soft constraints were imposed on refined atomic coordinates (Kirik, 1985) using the weight coefficients and taking into account the average values of corresponding distances and angles (Allen, 2002). At the final refinement step hydrogen atoms were rigidly attached to the respective carbons (Siemens, 1989). The resulting structural data have been deposited on CSD # 986013.

## II. RESULTS AND DISCUSSION

Redox equilibrium in the “Cysta-Cystea” system, occurring in living organisms, currently is not thoroughly studied, from the point of view of solvent type, the acidity of the medium, the influence of different type of metal ions, the solution composition in whole, and temperature (Foye and Kaewchansilp, 1979; Mark *et al.*, 1982; Carrillo *et al.*, 1989; Shaw *et al.*, 1991; Markello *et al.*, 1993; Steele and Opella, 1997; Wilson *et al.*, 2000; Allegra *et al.*, 2002; Kim *et al.*, 2002; Bharara *et al.*, 2005a; Louvain *et al.*, 2007; Eremin *et al.*, 2009). In most cases, the reaction condition changing leads to results far from expectations that makes impossible consistent description the set of transformations in “Cysta-Cystea”. Nevertheless, the study of Cysta and Cystea behavior under controlled conditions, the analysis of mutual transformations may provide necessary information for complete understanding of its chemical activity. The result of interaction of Cu(II) salt with dihydrochloride of cystamindi-ium in aqueous solution with an excess of hydrochloric acid according to the equation:



is investigated in this paper. Excess of hydrochloric acid inhibits  $[\text{CuCl}_4]^{2-}$  anion oxidation because of its low stability in neutral aqueous solution.  $\text{CystaH}_2^{2+}$  cations do not decompose in these conditions, resulting in the formation of the final product  $\text{CystaH}_2[\text{CuCl}_4]$ . Previously, such complex compounds containing  $\text{CystaH}_2^{2+}$  ion were prepared exclusively in organic media, particularly from ethanol solutions (Carrillo *et al.*, 1989). Thus, the correspondence between the acidity of the medium and solvent plays an essential role in the formation of the final product in this chemical transformation. The variation of one of the parameters may irreversibly affect the entire interaction of starting reagents.

According to the thermal analysis data the salt  $\text{CystaH}_2[\text{CuCl}_4]$  is stable in air up to 200  $^\circ\text{C}$  (Figure 1). Thermogravimetric (TG) and differential thermal analysis (DTA) curves show a multistage process of decomposition. The endothermic effect at 219  $^\circ\text{C}$  on the DTA curve (Figure 1) is accompanied by weight loss of 11.4(1)%. It allows suppose, that the salt transforms, with cystamine breaking on S–S bond and the release of one HCl molecule gives complex  $[\text{CuCl}_3(\text{NH}_2\text{CH}_2\text{CH}_2\text{S})](\text{NH}_3\text{CH}_2\text{CH}_2\text{S})$  at the first stage. At higher temperature this process is overlapped with

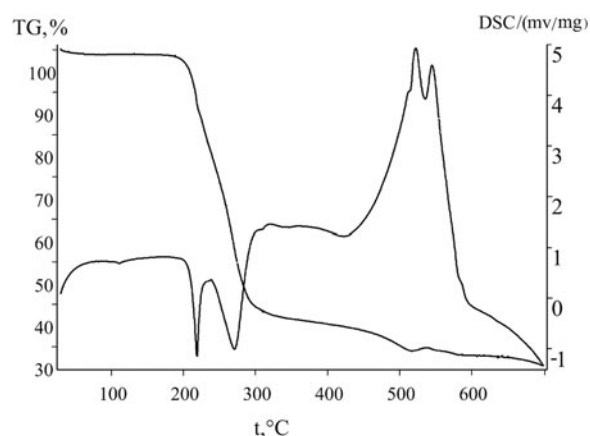
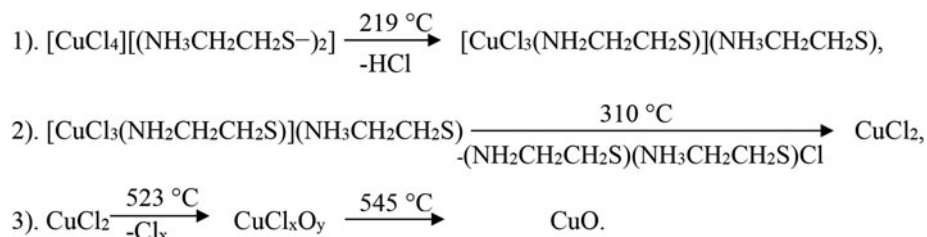


Figure 1. TG and DTA curves for  $\text{CystaH}_2[\text{CuCl}_4]$  salt.



Scheme 1. Stages of  $\text{CystaH}_2[\text{CuCl}_4]$  decomposition in air.

a significant substance disintegration including sublimation of the organic component with an additional weight loss of 51.2 (1)%. At 310 °C the copper dichloride  $\text{CuCl}_2$  is formed. In the range higher 300 up to 700 °C the process is described by the sloping graph of the mass loss and intense heat release. This is because of the gradual oxidation of  $\text{CuCl}_2$  by oxygen, which is accompanied by intensive heat release. Moreover, the DTA curve indicates a multi-stage oxidation process.  $\text{CuCl}_2$  turns to  $\text{CuCl}_x\text{O}_y$  and then at 545 °C – to  $\text{CuO}$  with the weight loss 19.8%. The stages of decomposition are presented in Scheme 1.

The IR spectra of  $\text{CystaH}_2[\text{CuCl}_4]$  salt and cystamine (Figure 2) do not contain significant differences thanks to the similar chemical condition of disulfide groups. The presence of S–S bonding in the structure of cystamine was confirmed by X-ray diffraction (XRD) (Kennard, 1965). Observed shifts of some bands are explained the different arrangement of hydrogen bonds. Slight shift of the bands at  $2900\text{--}3200\text{ cm}^{-1}$  [ $\nu(\text{N-H})$ ] and  $1560\text{--}1600\text{ cm}^{-1}$ , assigned to the deformation vibrations [ $\nu(\text{C-N})$ ], indicates a lack of metal atom coordination by  $\text{-NH}_3^+$  groups through nitrogen atoms.

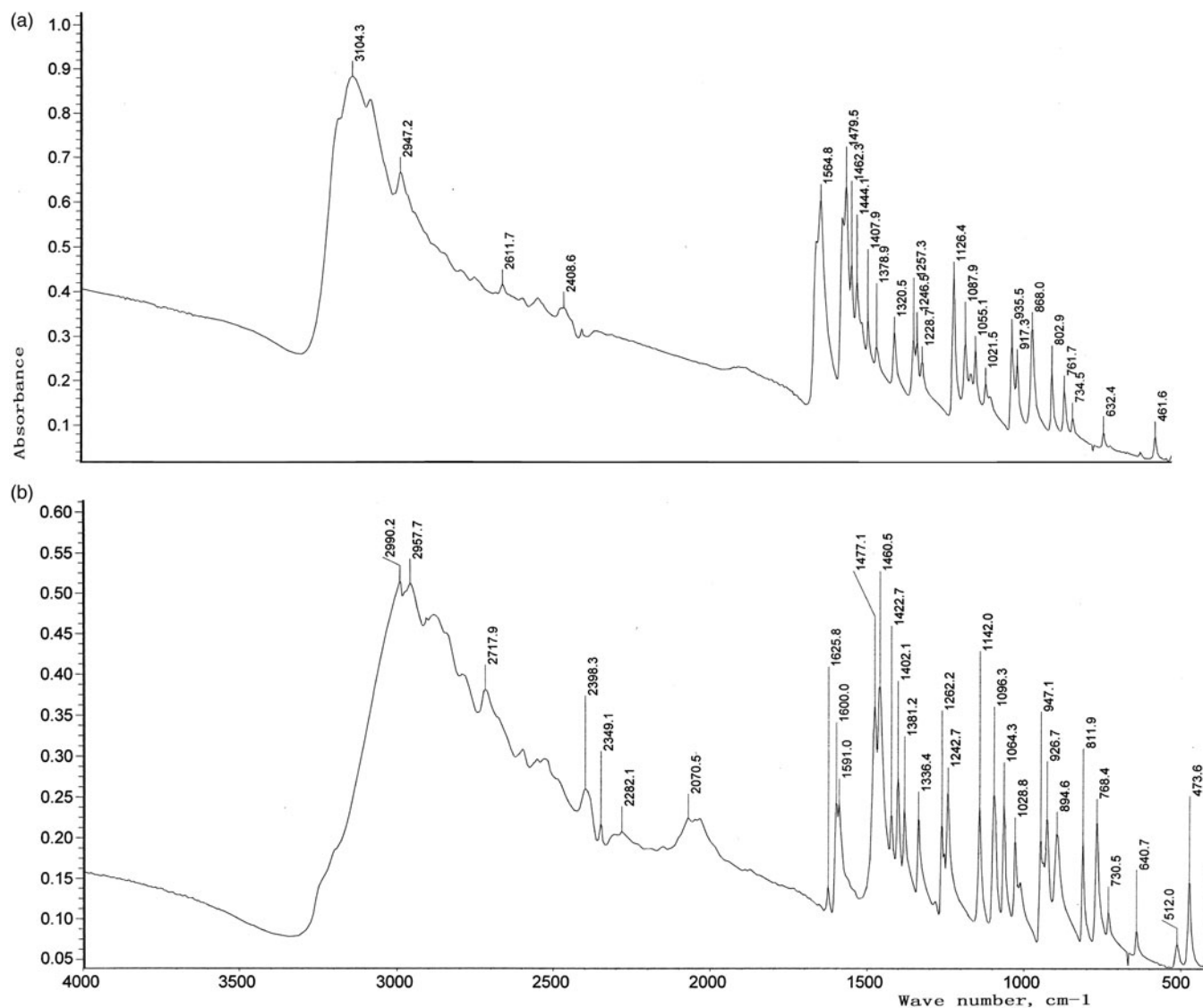


Figure 2. (a) IR spectra of  $\text{CystaH}_2[\text{CuCl}_4]$ . (b) IR spectra of cystamine  $\text{NH}_2(\text{CH}_2)_2\text{SS}(\text{CH}_2)_2\text{NH}_2$ .

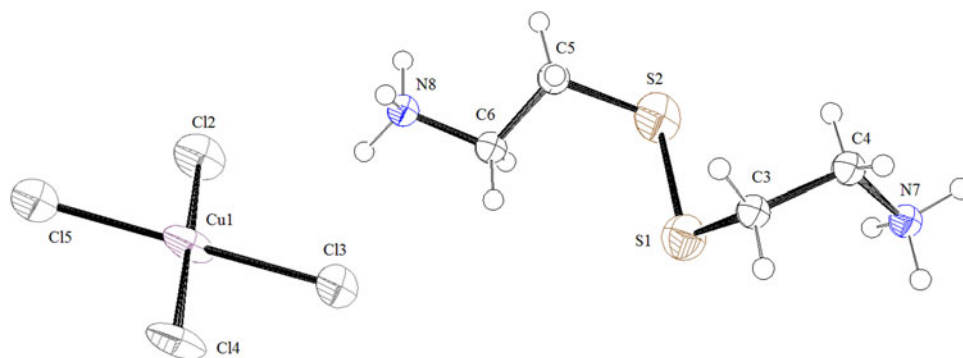


Figure 3. (Color online)  $[\text{CuCl}_4]^{2-}$  and  $\text{CystaH}_2^{2+}$  ions of the investigated compound  $\text{CystaH}_2[\text{CuCl}_4]$

This is also confirmed by the presence of bands at  $1447\text{--}1462$  and  $1578\text{--}1593\text{ cm}^{-1}$ , referred, to the symmetric deformation and degenerated deformation vibrations of  $-\text{NH}_3^+$  groups respectively. Reducing the length of C–S bond in  $\text{CystaH}_2[\text{CuCl}_4]$  leads to decreasing frequency of the stretched vibration up to  $632\text{ cm}^{-1}$  compared with the frequency  $[\nu(\text{C}–\text{S})]$  of the free ligand ( $768\text{ cm}^{-1}$ ) (Bharara *et al.*, 2005a). For lack of other bands in the region  $600\text{--}700$  and  $500\text{--}600\text{ cm}^{-1}$  can be explained by the absence of the Cu–S or Cu–N bonds (Foye and Kaewchansilp, 1979). The low-frequency oscillations at  $461\text{ cm}^{-1}$  are because of chemical metal–halogen bonds (Cu–Cl) (Sheludiyakova & Basova, 2002). Thus, on the basis of IR spectroscopic data it can be suggested that  $\text{CystaH}_2^{2+}$  cation presents in  $\text{CystaH}_2[\text{CuCl}_4]$  and there are no coordination of copper atoms by  $\text{CystaH}_2^{2+}$ .

Crystal structure of  $\text{CystaH}_2[\text{CuCl}_4]$  was determined by the X-ray powder diffraction technique. The modeling was performed taking into account the structures of the starting molecular fragments  $\text{CystaH}_2^{2+}$  и  $[\text{CuCl}_4]^{2-}$  (Figure 3) followed from the synthesis and chemical analyses. It was assumed that the complex anion  $[\text{CuCl}_4]^{2-}$  has a planar square structure typical for Cu(II).

Initially, the structure solution was obtained in the space group  $P2_1/a$ . After structure refinement this solution provided a good agreement between the calculated and experimental X-ray diffraction powder patterns ( $R_p = 5.04\%$ ,  $R_{wp} = 7.51\%$ ,  $R_{exp} = 4.81\%$ ,  $S = R_{wp}/R_{exp} = 1.56$ ). However, there were several unexplained reflexes about 1% of relative intensity, which were considered as impurities (Figure 4). It would be assumed that the center of symmetry in the space group  $P2_1/a$  connects two fragment of cystamine type ( $\text{NH}_3\text{CH}_2\text{CH}_2\text{S}-$ ) giving cystamindi-ium ion  $\text{CystaH}_2^{2+}$ . However, as it has been mentioned above, the main conformation of the cystamine molecule has no center of symmetry because of the specific configuration of the electronic system of (S–S) bond. This circumstance induced two hypotheses for testing. The first was that cystamindi-ium ion changed its conformation. The support for the hypothesis might be the fact of the specific interaction of cystamine with Cu(I) (Louvain *et al.*, 2008). The second was that the center symmetry was absent. The modeling performed in the group  $P2_1$  helped to solve the dilemma. It turned out that the reflexes forbidden in space group  $P2_1/a$  supplied a good explanation of “impurity” reflexes on the experimental X-ray powder pattern. This led to the unambiguous

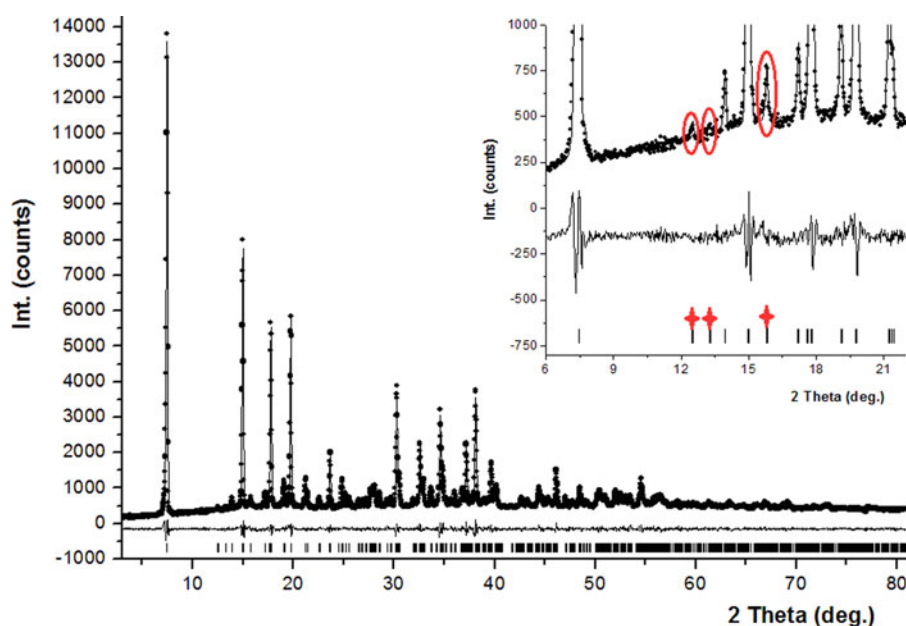


Figure 4. (Color online) – XRD patterns for  $\text{CystaH}_2[\text{CuCl}_4]$ : the experimental (dots) and calculated (solid line), the difference (solid line), position of calculated reflections in bottom. In the insertion, the part of the XRD pattern presented where the reflections forbidden in space group  $P2_1/a$ .

TABLE I. Crystallographic parameters and characteristics of X-ray powder diffraction structure determination for CystaH<sub>2</sub>[CuCl<sub>4</sub>].

Chemical formula	[NH <sub>3</sub> (CH <sub>2</sub> ) <sub>2</sub> SS(CH <sub>2</sub> ) <sub>2</sub> NH <sub>3</sub> ] [CuCl <sub>4</sub> ]
Molecular weight	359.66
Space group	<i>P</i> 2 <sub>1</sub>
<i>a</i> (Å)	7.183(1)
<i>b</i> (Å)	7.503(1)
<i>c</i> (Å)	12.009(1)
$\alpha$ (°)	90
$\beta$ (°)	101.18(1)
$\gamma$ (°)	90
<i>V</i> <sub>un.cell</sub> (Å <sup>3</sup> )	634.86
<i>Z</i>	2
<i>V</i> / <i>Z</i> (Å <sup>3</sup> )	317.43
$\rho$ <sub>calc.</sub> (g cm <sup>-3</sup> )	1.880
$\mu$ (mm <sup>-1</sup> )	12.943
<i>T</i> (K)	295
Diffractometer	X'Pert PRO
Radiation	CuK $\alpha$
$\lambda$ (Å)	$\lambda_1=1.54056, \lambda_2=1.54439$
Scanning area, $2\theta$ (°)	3.013–80.935
Number of points	2997
Number of reflections	421
<i>R</i> <sub>p</sub> (%)	3.67
<i>R</i> <sub>wp</sub> (%)	4.85
<i>R</i> <sub>exp</sub> (%)	4.00
<i>S</i> = <i>R</i> <sub>wp</sub> / <i>R</i> <sub>exp</sub>	1.21

choice of space group *P*2<sub>1</sub> (Figure 4). Only one possible orientation of cystamindi-ium ion was applied for the refinement. It allowed perceptible improving in X-ray powder diffraction fitting. The model with disordered ions was not applied because of the level of fitting was close to the statistical limit of reliability factors. Final crystallographic data and refinement characteristics are presented in Table I, and the atomic coordinates are listed in Table II. Figure 4 shows the diffraction data for CystaH<sub>2</sub>[CuCl<sub>4</sub>], including experimental and calculated X-ray powder diffraction patterns in comparison, the difference curve and the reflex positions.

The crystal structure of CystaH<sub>2</sub>[CuCl<sub>4</sub>] as the projection on (*bc*)-plane is shown in Figure 5, the main interatomic distances and angles are given in Table III. The structure has a layered type (Figure 5). Inorganic layers are built from [CuCl<sub>4</sub>]<sup>2-</sup> anions, which alternate with organic layers from protonated cystamine CystaH<sub>2</sub><sup>2+</sup> cations. The obtained crystal structure data confirm the presence of a disulfide bond S–S in the CystaH<sub>2</sub>[CuCl<sub>4</sub>] with a distance equal to 2.05(2) Å, indicating a lack of coordination CystaH<sub>2</sub><sup>2+</sup> ion to Cu(II). Localization CystaH<sub>2</sub><sup>2+</sup> cations between the complex anions [CuCl<sub>4</sub>]<sup>2-</sup>, as well as coordination of NH<sub>3</sub>-groups to the corresponding nucleophiles Cl<sup>-</sup> lead to the formation of hydrogen bonds. Each NH<sub>3</sub>-group forms three hydrogen bonds with two chlorine atoms belonging to the same complex

TABLE II. (a) Atomic coordinates of CystaH<sub>2</sub>[CuCl<sub>4</sub>].

Atom	<i>x/a</i>	<i>y/b</i>	<i>z/c</i>	<i>U</i> <sub>iso</sub>
Cu1	0.7368(1)	0.0980(1)	0.000 00	
Cl2	0.6769(1)	0.0627(1)	−0.1945(1)	
Cl3	0.9555(1)	0.3131(2)	−0.0134(1)	
Cl4	0.7966(1)	0.1332(1)	0.1945(2)	
Cl5	0.5181(1)	−0.1170(1)	0.0134(0)	
S1	0.7963(1)	0.4615(1)	0.5587(1)	
S2	0.8428(1)	0.7101(1)	0.498 33(1)	
C3	0.5509(1)	0.5090(1)	0.5723(1)	0.025 33
H3A	0.5025(11)	0.3986(13)	0.5954(10)	0.038 00
H3B	0.4720(11)	0.5432(13)	0.5016(10)	0.038 00
C4	0.5143(1)	0.6534(1)	0.6575(1)	0.025 33
H4A	0.3845(10)	0.6437(10)	0.6658(13)	0.038 00
H4B	0.5557(10)	0.7599(10)	0.6252(13)	0.038 00
C5	0.7597(1)	0.6664(1)	0.3442(1)	0.025 33
H5A	0.7796(10)	0.7741(12)	0.3048(10)	0.038 00
H5B	0.6280(10)	0.6344(12)	0.3257(10)	0.038 00
C6	0.8871(1)	0.5146(1)	0.3167(1)	0.025 33
H6A	0.8394(10)	0.4017(11)	0.3361(13)	0.038 00
H6B	1.0140(10)	0.5291(11)	0.3591(13)	0.038 00
N7	0.6357(1)	0.6303(2)	0.7728(1)	0.025 33
H7A	0.6123(11)	0.7269(1)	0.8209(11)	0.038 00
H7B	0.6038(11)	0.5195(1)	0.8049(11)	0.038 00
H7C	0.7669(11)	0.6295(1)	0.7865(11)	0.038 00
N8	0.8863(1)	0.5225(1)	0.1935(1)	0.025 33
H8A	0.9649(11)	0.4290(10)	0.1734(11)	0.038 00
H8B	0.7589(11)	0.5077(10)	0.1520(11)	0.038 00
H8C	0.9345(11)	0.6358(10)	0.1751(11)	0.038 00

(b). Anisotropic temperature parameters for some atoms of CystaH<sub>2</sub>[CuCl<sub>4</sub>].

Atom	<i>U</i> <sub>11</sub>	<i>U</i> <sub>22</sub>	<i>U</i> <sub>33</sub>	<i>U</i> <sub>12</sub>	<i>U</i> <sub>13</sub>	<i>U</i> <sub>23</sub>
Cu1	0.042(21)	0.021(45)	0.076(34)	0.000 00	0.040(51)	0.000 00
Cl2	0.025(30)	0.037(13)	0.052(12)	0.000 00	0.015(12)	0.000 00
Cl3	0.030(44)	0.050(11)	0.073(31)	0.000 00	0.024(13)	0.000 00
Cl4	0.031(23)	0.041(65)	0.051(41)	0.000 00	0.027(11)	0.000 00
Cl5	0.049(61)	0.017(19)	0.082(16)	0.000 00	0.018(10)	0.000 00
S1	0.048(13)	0.051(30)	0.050(12)	0.000 00	0.013(16)	0.000 00
S2	0.023(23)	0.064(20)	0.065(14)	0.000 00	0.020(19)	0.000 00

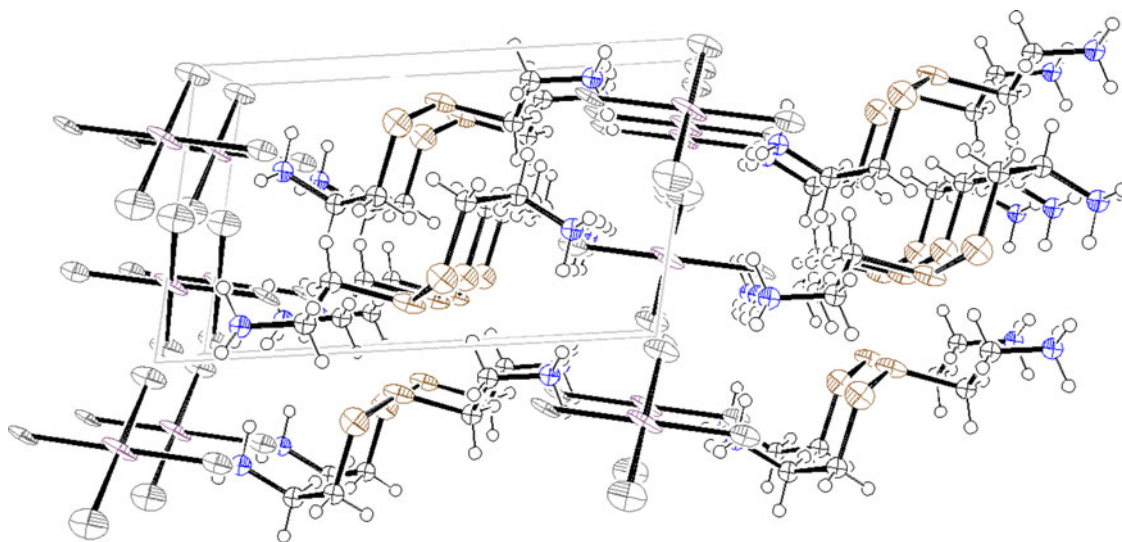


Figure 5. (Color online) The arrangement of the molecules in the unit cell of  $\text{CystaH}_2[\text{CuCl}_4]$  as the projection on the  $bc$  plane.

TABLE III. The most important interatomic distances and angles for  $\text{CystaH}_2[\text{CuCl}_4]$ .

Distance (Å)		Angle (°)		Torsion (°)	
Cu1–Cl2	2.31(1)	Cl3–Cu1–Cl2	90.3(1)	Cl2–Cl3–Cl4–Cu1	0.0(1)
Cu1–Cl3	2.28(1)	Cl2–Cu1–Cl5	89.7(1)	N8–C6–C5–S2	–157.1(1)
Cu1–Cl4	2.31(1)	Cl3–Cu1–Cl5	180.0(2)	C6–C5–S2–S1	–59.1(1)
Cu1–Cl5	2.28(1)	C3–S1–S2	94.6(1)	C5–S2–S1–C3	–88.9(1)
S1–C3	1.83(2)	S1–S2–C5	98.5(1)	S2–S1–C3–C4	–64.1(1)
C4–C3	1.54(1)	S2–C5–C6	104.7(1)	S1–C3–C4–N7	–49.5(1)
C4–N7	1.49(1)	C5–C6–N8	107.3(1)		
S2–C5	1.86(1)	S1–C3–C4	118.9(1)		
C5–C6	1.53(2)	C3–C4–N7	112.7(1)		
C6–N8	1.48(1)				
S1–S2	2.05(2)				

$[\text{CuCl}_4]^{2-}$ . The lengths of the hydrogen bonds are given in Table IV. Since each organic cation contains two amino groups on the opposite sides, this leads to the performing a retaining effect between the two anion layers (Figure 6). Compactness of the anionic layer is achieved by parquet package, which allows the occurrence of short contacts between the anionic copper complexes  $[\text{CuCl}_4]^{2-}$ . Chlorine atoms of neighboring anions are oriented along the axis of the square plane complex  $[\text{CuCl}_4]^{2-}$  at a distance of 2.80(1) and 3.05(2) Å completing it to a distorted octahedron,  $[\text{CuCl}_6]^{2-}$ , which is more typical for copper crystallochemistry (Figure 6). The lack of coordination between the metal and sulfur atoms was detected on the example of  $\text{CystaH}_2[\text{HgCl}_4]$  and described in detail in (Bharara *et al.*, 2005b). Saving S–S bonding was observed with the coordination centers as Pb, Bi, and V atoms (Pavani

*et al.*, 2006; Bi *et al.*, 2007; Louvain *et al.*, 2007). The coordination sphere around the central atoms in such compounds is formed by oxygen or halogen atoms. Some regularity in these structures can be formulated. The formation of anionic and

TABLE IV. The lengths of hydrogen bonds A–H...B in the structure of  $[\text{CuCl}_4][(\text{NH}_3\text{CH}_2\text{CH}_2\text{S}^-)_2]$ .

A–H...B	$d(\text{A}\cdots\text{B})$ (Å)
N7–H...Cl4	3.205(1)
N7–H...Cl2	3.27(4)
N8–H...Cl4	2.99(2)
N8–H...Cl3	3.06(1)
N8–H...Cl2	3.15(1)

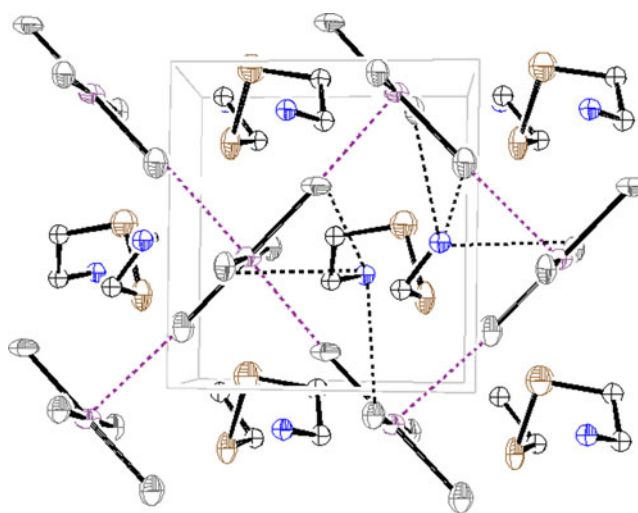


Figure 6. (Color online) The hydrogen bonding (dotted red lines) and the short contacts (dotted green lines) in the unit cell of  $\text{CystaH}_2[\text{CuCl}_4]$  in the projection to the  $(ab)$ -plane.

cationic blocks and their spatial segregation are occurred because of the possibility of additional coordination. In  $\text{CystaH}_2[\text{CuCl}_4]$ , anionic tetrachloride copper complexes form the layers, in which the copper plane coordination is completed to octahedral by chlorine atoms from neighboring complexes. Similar complexes may be localized on the symmetric positions (on symmetry elements), which is the characteristic for the compounds of Cu and Hg, or independently of the cell volume for Pb and V (Pavani *et al.*, 2006; Louvain *et al.*, 2007). Secondly, there is an additional energy gain because of the formation of hydrogen bonds, leading to the stabilization of a particular structural adjustment. Note that in most of the known compounds wherein there is no coordination between the sulfur and metal atoms, there are twice as much hydrogen bonding between counterions, than in the presence of such coordination. In most cases in compounds with coordination of the metal atom to sulfur, two sulfur atoms involved into the coordination. It leads to the formation of stable organometallic five- or six-membered rings. Typically, these fragments are formed in the less symmetric structures, when the additional coordination causes increased stabilization of the compound.

In conclusion, the interaction of copper(II) dichloride with cystamindi-ium dihydrochloride investigated in the strong acid medium. The reaction results in the formation of the complex compound  $[\text{NH}_3(\text{CH}_2)_2\text{SS}(\text{CH}_2)_2\text{NH}_3][\text{CuCl}_4]$ , which crystallizes in the form of fine polycrystalline powder. According to IR spectroscopy and X-ray powder diffraction analyses, a disulfide bond (S–S) presents in the compound. Complex salt  $[\text{NH}_3(\text{CH}_2)_2\text{SS}(\text{CH}_2)_2\text{NH}_3][\text{CuCl}_4]$  is stable in air up to 200 °C, and then decomposes in several steps under heating with changing the coordination sphere of copper. The compound has ionic structure with packing of the  $[\text{CuCl}_4]^{2-}$  and  $\text{CystaH}_2^{2+}$  ions in the form of layers in the cell. Additional retention between cationic and anionic layers occurs through the formation of hydrogen bonding between the  $\text{NH}_3$ -groups and chlorine atoms of the  $[\text{CuCl}_4]^{2-}$  complex. An additional stabilization factor is the parquet such as anion parking, which provides additional coordination for copper atoms transforming square-planar to a distorted octahedral coordination.

## ACKNOWLEDGEMENTS

The authors are grateful to the reviewer for valuable comments, which allowed significantly improve the results. The study was conducted according to the SFU state assignment of RF Ministry of Science and Education in 2014, with financial support ICDD (Grant-in-Aid #10-93).

## SUPPLEMENTARY MATERIAL

The supplementary material for this article can be found at <http://www.journals.cambridge.org/PDJ>

- Allegra, P., Amodeo, E., and Colombatto, S. (2002). "The ability of cystamine to bind DNA," *Amino Acids* **22**, 155–166.
- Allen, F. H. (2002). "The Cambridge Structural Database: a quarter of a million crystal structures and rising," *Acta Crystallogr. B* **58**, 380–388.
- Bharara, M. S., Bui, T. H., Parkin, S., and Atwood, D. A. (2005a). "Mercurophilic interaction in novel polynuclear Hg(II)-2-aminoethanethiolates," *Dalton Trans.* **24**, 3874–3880.

- Bharara, M. S., Parkin, S., and Atwood, D. A. (2005b). "Solution behavior of Hg(II)-cystamine by UV–Vis and  $^{199}\text{Hg}$  NMR," *Main Group Chem.* **4**, 217–225.
- Bi, W., Louvain, N., Mercier, N., Luc, J., and Sahraoui, B. (2007). "Type structure, which is composed of organic diammonium, triiodide and hexa-iodobismuthate, varies according to different structures of incorporated cations," *Cryst. Eng. Commun.* **9**, 298–303.
- Bi, W., Louvain, N., Mercier, N., Luc, J., Rau, I., Kajzar, F., and Sahraoui, B. (2008). "A switchable NLO organic-inorganic compound based on conformationally chiral disulfide molecules and Bi(III)-5 iodobismuthate networks," *Adv. Mater.* **20**, 1013–1017.
- Carrillo, D., Gouzerh, P., and Jeannin, Y. (1989). "Disulfide bond cleavage in the Nickel(II)-cystamine and copper(II)-cystamine systems. X-ray crystal structure of  $\text{trans}[\text{Ni}(\text{SCH}_2\text{CH}_2\text{NH}_2)_2]$ ," *Polyhedron* **8**, 2837–2840.
- Eremin, A. V., Antonov, V. G., and Panina, N. S. (2009). "Coordination compounds of palladium and iron with oxygen-bridged ligands involved in the oxidation of thioamino acids," *Rossiiskii. Khim. J.* **53**, 135–139.
- Favre-Nicolin, V. and Černý, R. (2002). "FOX, 'free objects for crystallography': a modular approach to *ab initio* structure determination from powder diffraction," *J. Appl. Crystallogr.* **35**, 734–743.
- Foye, W. O. and Kaewchansilp, V. (1979). "Mercaptoalkylamine coordination compounds of platinum(II) and palladium(II) and their anticancer activity," *J. Pharm. Sci.* **68**, 1131–1135.
- Kennard, O. (1965). *Cambridge Structural Database (Database)* (University of Cambridge, Cambridge, UK).
- Kim, C. H., Parkin, S., Bharara, M., and Atwood, D. (2002). "Linear coordination of Hg(II) by cysteamine," *Polyhedron* **21**, 225–228.
- Kirik, S. D. (1985). "Refinement of the crystal structures along the powder pattern profile by using rigid structural constraints," *Kristallographia* **30**, 185–187.
- Kirik, S. D., Borisov, S. V., and Fedorov, V. E. (1981). "Program for crystal structure refinement using X-ray powder pattern," *Zh. Strukt. Khim.* **22**, 131–135.
- Louvain, N., Bi, W., and Mercier, N. (2007). " $\text{PbnI}4n + 2(2n + 2)$ – Ribbons ( $n = 3, 5$ ) as dimensional reductions of 2D perovskite layers in cystamine cation based hybrids, also incorporating iodine molecules or reversible guest water molecules," *Dalton Trans.* **9**, 965–970.
- Louvain, N., Mercier, N., and Kurmoo, M. (2008). "Cu–I–Br oligomers and polymers involving Cu–S(cystamine) bonds," *Eur. J. Inorg. Chem.* **10**, 1654–1660.
- Mark, H. F., Othmer, D. F., Overberger, C. G., and Seaborg, G. T. (1982). *Kirk-Othmer Encyclopedia of Chemical Technology* (Wiley, New York), 3rd ed., Vol. **19**, p. 801.
- Markello, T. C., Bernardini, I. M., and Gahl, W. A. (1993). "Improved renal function in children with cystinosis treated with cysteamine," *Engl. J. Med.* **328**, 1157–1162.
- Pavani, K., Upreti, S., and Ramanan, A. (2006). "Two new polyoxovanadate clusters templated through cysteamine," *J. Chem. Sci.* **118**, 159–164.
- Rodríguez-Carvajal, J. (2009). FullProf, version 4.06 (Computer Software), IUCr Software.
- Shaw, C. F., Stillman, M. J., and Suzuki, K. T. (1991). *Metallothioneins: Synthesis, Structure and Properties of Metallothioneins, Phytochelatins and Metal-Thiolate Complexes* (VCH Publishers, New York), pp. 1–13.
- Sheludyakova, L. A. and Basova, T. V. (2002). "Hexachlorocuprate (II) anion: the vibrational spectra and structure," *J. Struct. Khim.* **43**, 629–633.
- Siemens (1989). XP. Molecular Graphics Program, version 4.0 (Computer Software), Siemens Analytical X-ray Instruments Inc., Madison, Wisconsin, USA.
- Solovyov, L. A. and Kirik, S. D. (1993). "Application of simulated annealing approach in powder crystal structure analysis," *Mater. Sci. Forum* **133**–136.
- Steele, R. A. and Opella, S. J. (1997). "Structures of the reduced and mercury-bound forms of MerP, the periplasmic protein from the bacterial mercury detoxification system," *Biochemistry* **36**, 6885–6895.
- Visser, J. W. (1969). "A fully automatic program for finding the unit cell from powder data," *J. Appl. Crystallogr.* **2**, 89–95.
- Wilson, J. R., Leang, C., Morby, A. P., Hobman, J. L., and Brown, N. L. (2000). "MerF is a mercury transport protein: different structures but a common mechanism for mercuric ion transporters?" *FEBS Lett.* **472**, 78–82.